Effects Of Permeability and Pore Connectivity On Gas Trapping In Carbonate Rocks

Caroline H. Dias[1], Carlos C. Júnior[1], Matheus G. Ramirez[1], Felipe Eler[1], Maira Lima[1], Paulo Couto[1]

[1]*Department of Civil Engineering, COPPE, Federal University of Rio de Janeiro*
caroldias@petroleo.ufrj.br

Abstract. Trapped gas is a significant factor affecting the hydraulic properties of oil reservoirs, including recoverable oil reserves. The degree of trapped gas in oil fields is a crucial aspect that affects the convergence of recoverable reserves, which has been evaluated in different experimental and simulation studies. These studies aim to assess the impact of trapped gas on different rock properties, as it is crucial for the Advanced Oil Recovery (EOR) and Carbon Capture, Use and Storage (CCUS) scenarios. several studies show that air or gas entrapment is a function of many parameters, including the prevailing wetting rate, wettability, and especially grain texture and pore structure. Understanding and quantifying the effects of trapped gas in oil reservoirs is challenging, particularly for carbonate rocks that have an unusually complex multiscale heterogeneous pore structure, causing fluid retention and unique flow properties. the same is not observed for carbonate rocks. This study examined how permeability and pore connectivity interact to influence saturation levels of trapped gas in 47 representative samples of carbonate rock formations. The 3D characterization of the pore space was made possible through microCT images, obtained for the silurian dolomite and coquina samples. It has been observed that larger pore radii and better connectivity lead to increased gas trapping, even in cases where pore connectivity may be more pronounced. This contrasted with previous assumptions emphasizing the influence of pore structure on gas trapping.

Keywords: Gas trapping saturation, Permeability, Pore connectivity, CCUS, EOR.

1 Introduction

Gas trapping in porous media occurs during displacement of an initially present non-wetting phase by an infiltrating wetting phase [1, 2]. Gas trapping plays an important role also in hydrocarbon recovery and carbon capture and storage (CCS) processes [3]. Regarding hydrocarbon recovery efficiency, capillary trapping of gas reduces residual oil saturation [4]. In case of CCS, the main objective is to maximize capillary trapping to increase CO_2 storage [5]. These various studies show that air or gas trapping is a function of many parameters, including the prevailing wetting rate, wettability, and especially grain texture and pore structure.

Understanding and quantifying the effects of trapped gas in oil reservoirs is a challenge, particularly for carbonate rocks which have an unusually complex multiscale heterogeneous pore structure causing unique fluid retention and flow properties [6]. Carbonate hydrocarbon reservoirs, including the Brazilian Pre-Salt, are the subject of several scientific investigations due to their geological complexity and economic value [7].

One of the main uncertainties in estimating recoverable reserves of oil fields is the large variation in observed values of trapped gas saturation (S_{gt}). Various experimental and simulation studies have been conducted to assess how selected porous media properties affect the degree of gas trapping [8]. Pore structure and pore connectivity play especially a key role in the gas trapping process. The coordination number (or pore connectivity) represents the number of pore bodies that are connected with adjacent pores, gas trapping is favored when wide pores are connected to narrow throats, with a well-connected pore system disfavoring gas trapping [9]. Fatemi and Sohrabi [10] verified the influence of wettability on gas trapping. They observed that wettability to water leads to more gas trapping, probably due to increased snap-off in such systems. Kazemi et al. [11], among others, found that trapped gas saturation (S_{gt}) tended to increase with initial gas saturation (S_{gi}).

Compared to sandstones, there has been relatively limited research focused on gas trapping within carbonate rocks. In a study conducted by Tanino and Blunt [1], the impact of pore structure on capillary trapping was assessed

in both sandstone and carbonate samples. Their findings revealed that capillary trapping predominantly increased with higher pore body-to-throat aspect ratios but tended to decrease with elevated pore coordination numbers. They also attempted to correlate trapped saturation with the microporosity fraction of the pore volume, although this relationship did not consistently hold. Interestingly, the microporosity within their samples exhibited similar pore aspect ratios and connectivity to the macroporosity region.

Another study by Khisamov et al. [12] introduced a method for estimating trapped gas saturation based on quantitative pore space characteristics and wettability. They observed that the ratio of pore bodies to pore throats played a pivotal role in controlling the trapping capacity of carbonate samples. Additionally, they demonstrated that carbonate rocks with larger pores, particularly when water-wet, exhibited higher levels of trapped gas saturations.

Pentland [13] compiled data illustrating the relationship between S_{gt} (trapped gas saturation) and permeability. Notably, permeability was presented in units of (m^2), with a conversion factor to mD being $9.87E^{-16}\ m^2$. The author highlighted that samples with greater porosity generally exhibited higher permeabilities, and such samples with higher permeabilities tended to have lower aspect ratios and increased pore connectivity, which reduced trapping via snap-off. It's important to note that the correlation between permeability and S_{gt} was found to be weaker compared to the relationship between porosity and S_{gt}.

In the recent study by Dias et al. [14], a significant revelation emerged regarding the profound influence of pore characteristics on the complex processes governing gas entrapment within carbonate rock formations. Furthermore, these distinctive pore features intricately shape the hydraulic properties during multiphase flow, ultimately impacting the recoverable oil reserves within carbonate rock reservoirs. To delve deeper into the properties influencing trapped gas saturation, this study aims to investigate how permeability and pore connectivity interact to affect trapped gas saturation levels within representative samples of carbonate rock formations.

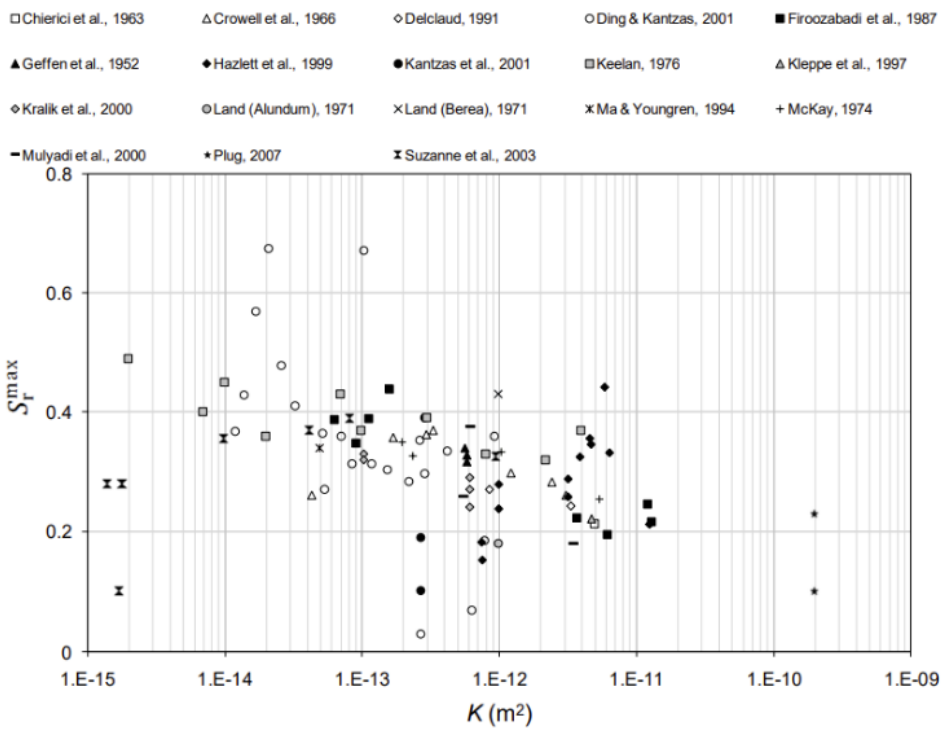

Figure 1. Effect of permeability on residual saturation for different data of the literature (extracted from Pentland [13]).

2 Materials and Methods

For the analysis of trapped gas saturation, 47 samples from 4 different carbonate lithologies were selected. The experiments in different lithologies aim to provide a representative database for each rock type. Among the selected carbonate rocks, there are the coquinas of the Morro do Chaves Formation (Sergipe-Alagoas Basin) and the travertines of Tivoli in Italy (Acque Albule Basin). These carbonates have been gaining ground in the oil geology scenario due to the possibility of being analogous to the facies present in the Brazilian pre-salt fields. The Figure 2 presents a selection of representative samples for each group of analyzed carbonate rocks

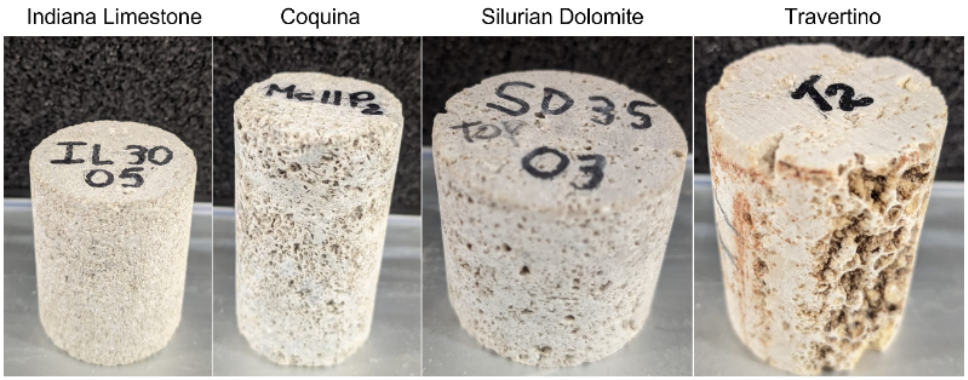

Figure 2. Selection of representative samples for each group of carbonate rocks analyzed

Procedures for estimating followed closely the approach described by Aissaoui [15]. Samples (5.0 cm long and 3.8 cm in diameter) were kept first for 24 hours in a controlled humidity oven at (60 °C and a relative humidity of 40%) to ensure completely dry plugs with air saturations at of near 100%. Coreflood tests were subsequently performed to determine air-water S_{gt} values by imbibing water under laboratory conditions. We used a confining pressure of 1,000 psi (6.89 MPa) and ambient fluid pressures, with the temperature being 21 °C. The experimental apparatus comprised a positive displacement pump, a confinement cell, pressure differential measurement transducers, graduated glassware, and an image capture system (Figura 3). After inserting the sample into the core holder, the confining pressure was raised to 1,000 psi (6.89 MPa, the same confining pressure used to measure the routine core properties). A positive displacement pump was used to inject distilled water into the system at a flow rate of 1 cm³/min. The distilled water was carefully deaerated to ensure that no gas was injected into the sample and during the imbibition. The gas initially contained in the dry samples was displaced and collected at the equipment outlet during a period of 24 hours. This information was recorded, along with the time and temperature at which production occurred, to yield estimates of S_{gt} .

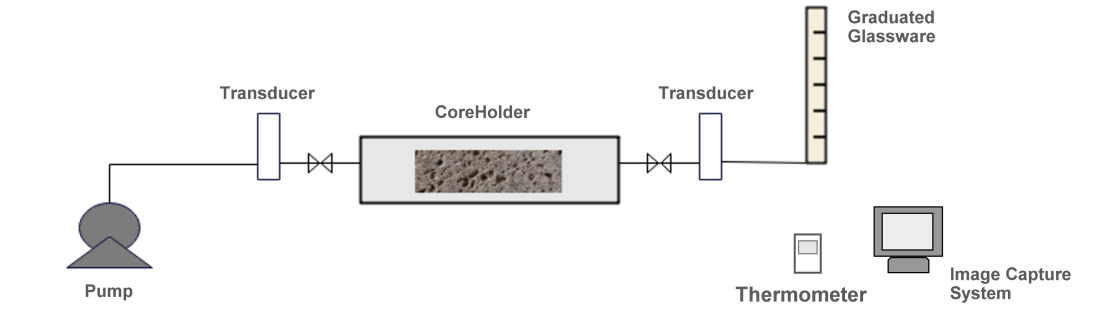

Figure 3. Experimental setup used for the trapped gas (S_{gt}) measurements.

2.1 X-ray microtomography (microCT)

The acquisitions of the images analyzed in this research were carried out with the CoreTOM equipment (Tescan/XRE). The images made possible investigations of the structure of pores on a micrometer scale possible thanks to the ability of radiation to penetrate materials and detect them in different degrees. The images made possible investigations of the structure of pores on a micrometer scale possible thanks to the ability of radiation to penetrate materials and detect them in different degrees.

Image segmentation into pores and mineral matrix from microCT images of coquina sample at voxel size 25µm (Figure 4) was performed using the threshold tool. After the segmentation step, tools in the Avizzo software are used in order to allow the porous space, visualized in the images, to be transformed into a set of cylindrical tubes (equivalent to pore throats) and spheres (equivalent to pore bodies) called skeleton. This transformation into tubes and spheres providing a 3D file with these characteristics, provides a spreadsheet with the topology of the

skeleton. comprising the nodes (connections in pore bodies), points (pores with location and radius) and segment (throat pores) of the connected clusters.

The PoreStudio [16] software was used in this research to model the porous system, enabling a quantitative understanding of the entire system. The software uses multidirectional pore modeling to simulate flow, where the numerical scheme is based on the assumption that porous media can be represented by a network of pore bodies and throats with finite volume.

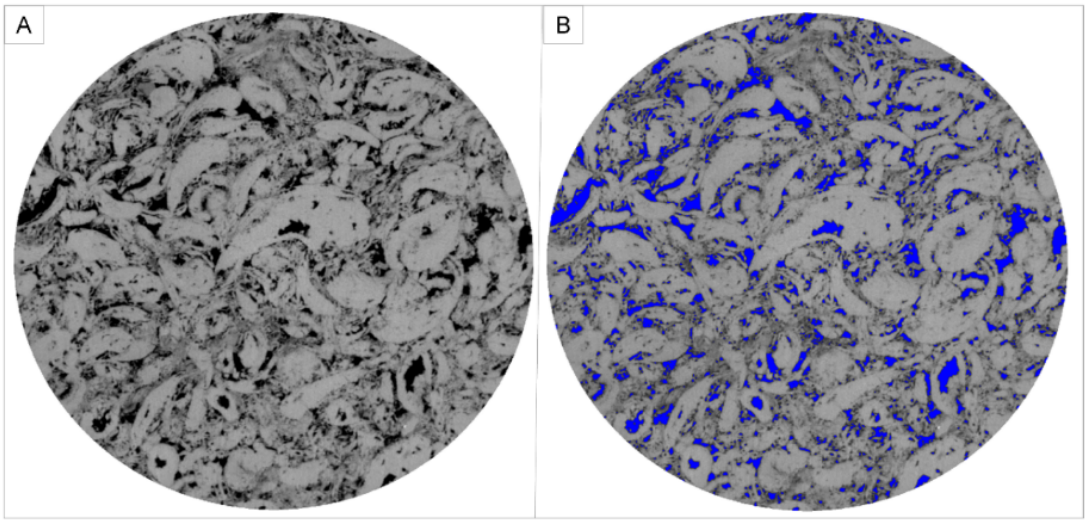

Figure 4. (A) Grayscale image with black pores and gray rock matrix; (B) Grayscale image with segmented pores in blue

3 Results

In the course of this research, we examined a diverse set of samples, each displaying a wide range of porosity, ranging from 6.0% to 43.8%, and permeability, which varied from 1.70 mD to 1737 mD. Figure 5 visually presents the correlation between porosity and permeability values. The graph effectively showcases a spectrum of porous media, encompassing materials that facilitate fluid flow and others that exhibit greater resistance, as indicated by their low permeability.

To further explore the relationship between permeability and S_{gt}, we constructed a graphical representation, as depicted in Figure 6. The resulting linear equation yielded a correlation coefficient (R2) of 0.2785, suggesting a relatively weak association between these properties. Despite the scattered data points, a subtle trend is discernible - higher S_{gt} values tend to align with increased permeability. This observation contrasts with the trend identified in the findings of Pentland [13], as illustrated in Figure 1.

Investigating the influence of pore connectivity on the interplay between permeability and S_{gt}, we selected two samples: a Silurian dolomite sample with a 60% S_{gt} and a coquina sample with a 40% S_{gt}. Figure 7 illustrates the Coordination number versus frequency values, revealing that the Silurian dolomite sample exhibits superior pore connectivity compared to the coquina sample. Interestingly, the coquina sample displays a higher frequency of connected pores, with some having up to 7 throats.

A more nuanced analysis of pore connectivity is achieved through a graph plotting pore frequency against connection number for varying pore radii (Figure 8). In the case of smaller pore radii, the coquina sample exhibits higher frequency across all coordination numbers. However, as the pore radius increases, the Silurian dolomite sample dominates in terms of frequency, regardless of the coordination number. Drawing parallels with the S_{gt} values, we observe that samples with gas entrapment tend to have larger pore radii and enhanced pore connectivity.

This phenomenon aligns with the findings of Blunt and Scher [17], who postulated that during water-wettable rock imbibition, water films proliferate in throats and along pore walls under rising water pressure. This process continues until the non-wetting phase (in this context, gas) loses contact with the solid surface. Consequently, engulfed throats become inundated by the wetting fluid, while the non-wetting phase remains trapped within porous structures, leading to substantial entrapment within these pores. This essentially houses the bulk of the void volume within the rock, as explained by [9].

It's noteworthy that despite the Silurian dolomite sample exhibiting enhanced pore connectivity compared

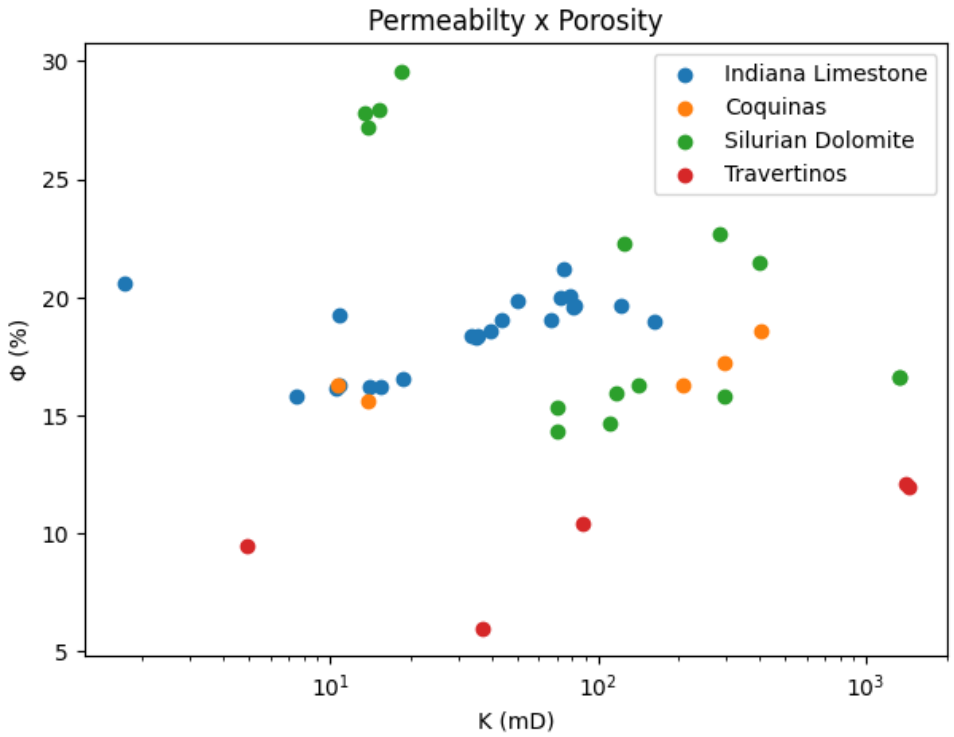

Figure 5. Graph of permeability versus porosity for the 47 carbonate samples analyzed.

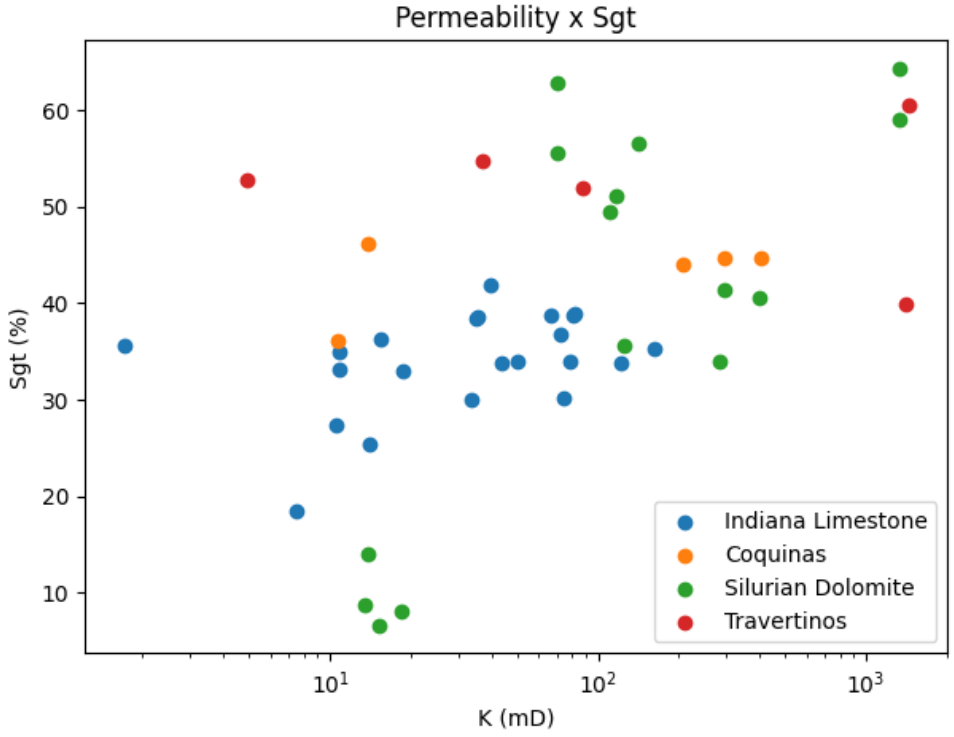

Figure 6. Graph of permeability versus S_{gt} for the 47 carbonate samples analyzed.

to the coquina sample (a condition that might be expected to hinder gas entrapment), the preponderance of larger pores in its structure played a decisive role in favoring greater gas entrapment relative to the coquina sample. Therefore, contrary to the findings of Pentland [13], we find that pore connectivity only adversely impacts gas

entrapment when the porous structure does not have a more substantial influence, as is the case with micropores

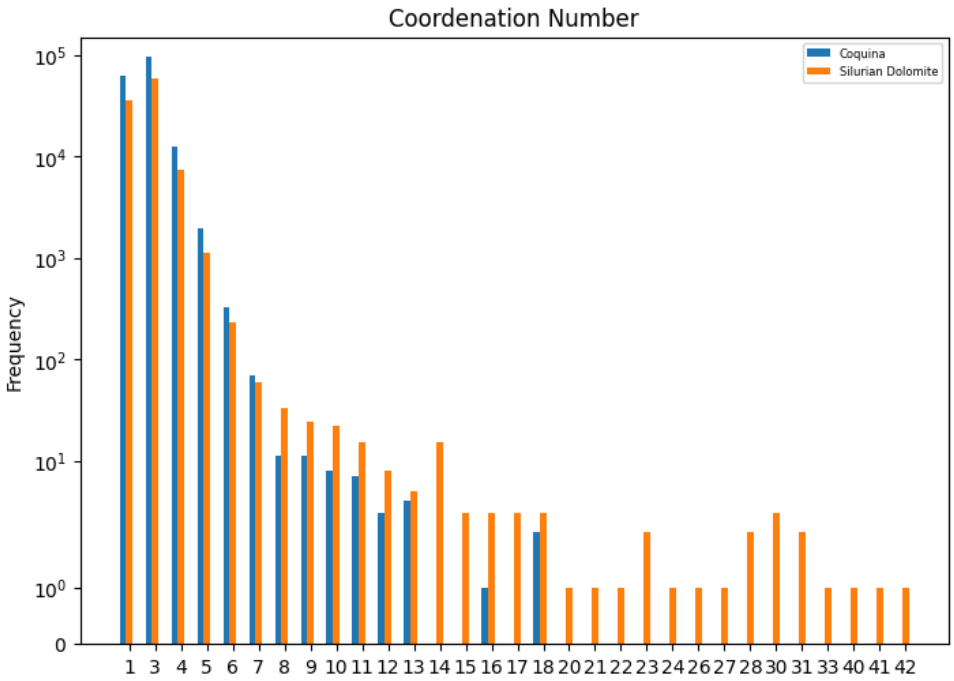

Figure 7. Comparison of coordination numbers by frequency of silurian dolomite and coquina samples.

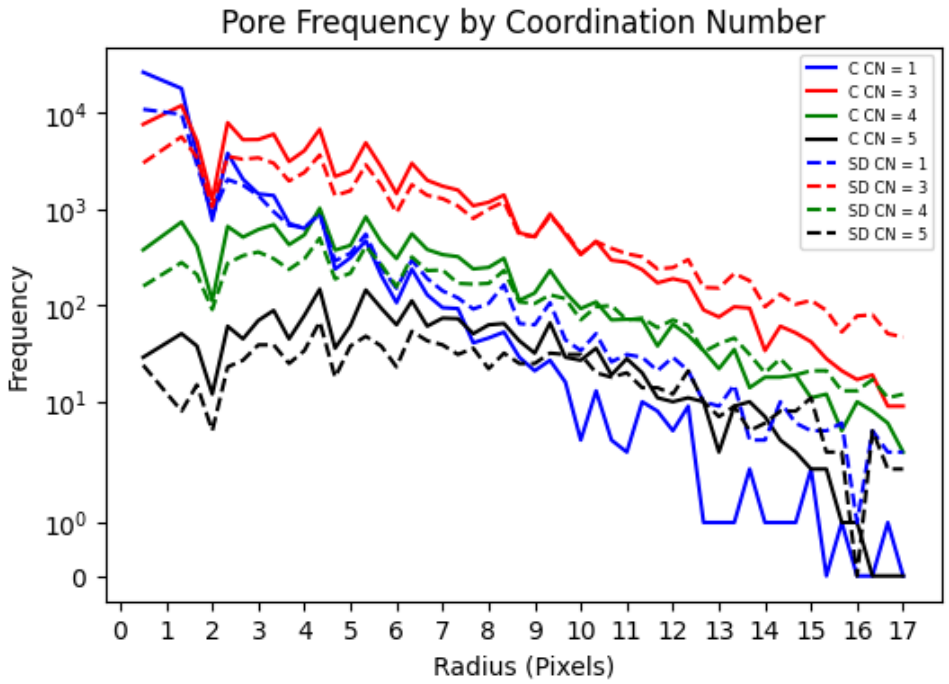

Figure 8. Pore frequency by coordination number for different pore sizes for silurian dolomite and coquina sample.

4 Conclusions

This research examined a diverse set of samples with different ranges of porosity and permeability. The correlation between porosity and permeability showed a spectrum of porous media with different fluid flow characteristics. Analysis of the relationship between permeability and Sgt (specific gas trapping) showed a weak correlation, contrary to previous findings. The impact of pore connectivity on permeability and Sgt was investigated across selected samples, revealing the role of connectivity in gas trapping. The 3D characterization of the pore space using microCT images provided an attractive means of explaining the high S_{gt} values obtained for the silurian dolomite and coquina samples. The study found that larger pore radii and improved connectivity lead to increased gas trapping, even in cases where pore connectivity may be more pronounced. This contrasted with previous assumptions, emphasizing the influence of pore structure on gas trapping.

Acknowledgements. This research was carried out in association with ongoing R&D projects registered as ANP 19027-2, "Desenvolvimento de infraestrutura para pesquisa e desenvolvimento em recuperação avançada de óleo – EOR no Brasil" (UFRJ/Shell Brasil/ ANP) setting-up a advanced EOR Lab facility for R&D in Brasil, and ANP 20163-2, "Análise experimental da recuperação de petróleo para as rochas carbonáticas do pré-sal brasileiro através da injeção alternada de CO2 e água", sponsored by Shell Brasil under the ANP R&D levy as "Compromisso de Investimentos com Pesquisa e Desenvolvimento". This study was financed in part by the Coordenação de Aperfeiçoamento de Pessoal de Nível Superior- Brasil (CAPES) - Finance Code 001 and carried out with the support of CNPq (National Council of Scientific and Technological Development, Brazil). We also thank the research teams of LRAP/COPPE/UFRJ.

References

[1] Y. Tanino and M. J. Blunt. Capillary trapping in sandstones and carbonates: Dependence on pore structure. *Water Resources Research*, vol. 48, n. 8, 2012.

[2] S. Mohammadian, H. Geistlinger, and H.-J. Vogel. Quantification of gas-phase trapping within the capillary fringe using computed microtomography. *Vadose Zone Journal*, vol. 14, n. 5, 2015.

[3] S. Wang, T. K. Tokunaga, J. Wan, W. Dong, and Y. Kim. Capillary pressure-saturation relations in quartz and carbonate sands: Limitations for correlating capillary and wettability influences on air, oil, and supercritical co2 trapping. *Water Resources Research*, vol. 52, n. 8, pp. 6671–6690, 2016.

[4] S. Afzali, N. Rezaei, and S. Zendehboudi. A comprehensive review on enhanced oil recovery by water alternating gas (wag) injection. *Fuel*, vol. 227, pp. 218–246, 2018.

[5] L. Ruspini, R. Farokhpoor, and P. Øren. Pore-scale modeling of capillary trapping in water-wet porous media: A new cooperative pore-body filling model. *Advances in Water Resources*, vol. 108, pp. 1–14, 2017.

[6] W. Godoy, E. M. Pontedeiro, F. Hoerlle, A. Raoof, M. T. Van Genuchten, J. Santiago, P. Couto, and others. Computational and experimental pore-scale studies of a carbonate rock sample. *Journal of Hydrology and Hydromechanics*, vol. 67, n. 4, pp. 372–383, 2019.

[7] M. C. Lima, E. M. Pontedeiro, M. G. Ramirez, J. Favoreto, dos H. N. Santos, van M. T. Genuchten, L. Borghi, P. Couto, and A. Raoof. Impacts of mineralogy on petrophysical properties. *Transport in Porous Media*, vol. 145, n. 1, pp. 103–125, 2022.

[8] G. Jerauld. Prudhoe bay gas/oil relative permeability. *SPE Reservoir Engineering*, vol. 12, n. 01, pp. 66–73, 1997.

[9] S. Krevor, M. J. Blunt, S. M. Benson, C. H. Pentland, C. Reynolds, A. Al-Menhali, and B. Niu. Capillary trapping for geologic carbon dioxide storage–from pore scale physics to field scale implications. *International Journal of Greenhouse Gas Control*, vol. 40, pp. 221–237, 2015.

[10] S. M. Fatemi and M. Sohrabi. Experimental and theoretical investigation of oil and gas trapping under two- and three-phase flow including water alternating gas (wag) injection. In *SPE Annual Technical Conference and Exhibition?*, pp. D021S030R005. SPE, 2013.

[11] F. Kazemi, R. Azin, and S. Osfouri. Evaluation of phase trapping models in gas-condensate systems in an unconsolidated sand pack. *Journal of Petroleum Science and Engineering*, vol. 195, pp. 107848, 2020.

[12] R. Khisamov, V. Bazarevskaya, I. Burkhanova, V. Kuzmin, M. Bolshakov, and O. Marutyan. Influence of the pore space structure and wettability on residual gas saturation. *Georesour*, vol. 22, n. 2, pp. 2–7, 2020.

[13] C. H. Pentland. Measurements of non-wetting phase trapping in porous media, 2011.

[14] C. H. Dias, F. M. Eler, C. Cordeiro, M. G. Ramirez, J. A. Soares, D. Nunes, M. C. Lima, and P. Couto. Effects of pore size and pore connectivity on trapped gas saturation. *Journal of Hydrology and Hydromechanics*, vol. 71,

n. 1, pp. 11–21, 2023.
[15] A. Aissaoui. Etude théorique et expérimentale de l'hystérésis des pressions capillaries et des perméabilitiés relatives en vue du stockage souterrain de gaz. *Ecole des Mines de Paris, Paris*, 1983.
[16] A. Raoof, H. M. Nick, S. M. Hassanizadeh, and C. Spiers. Poreflow: A complex pore-network model for simulation of reactive transport in variably saturated porous media. *Computers & Geosciences*, vol. 61, pp. 160–174, 2013.
[17] M. J. Blunt and H. Scher. Pore-level modeling of wetting. *Physical review E*, vol. 52, n. 6, pp. 6387, 1995.